

IMPROVED LOUDSPEAKER ARRAY MODELING

David W. Gunness & William R. Hoy

Eastern Acoustic Works, Inc.
Whitinsville, MA USA

ABSTRACT

Measurements of directional response are often used to predict interactions in arrays. Implicit in this approach is a simplistic source model with demonstrable limitations. The source models can be greatly improved by incorporating the known physical attributes of the horns. Example models of horn directionality are presented which agree closely with measured data, and which accurately predict array performance.

0 INTRODUCTION

0.1 Standard Practice

The practice of modeling acoustical spaces in software has become commonplace. Acoustical modeling programs enable designers to evaluate loudspeaker performance in a given space, whether or not the space already exists. Determinations can be made regarding coverage, maximum SPL, intelligibility, preferred source location and aiming, and other relevant parameters. Practically any project warranting the effort of constructing architectural models will involve multiple loudspeakers, whether for the purpose of achieving adequate coverage or sufficient SPL. A weakness of the modeling process is that the calculation of interactions suffers from significant inaccuracy.

This inaccuracy is not the fault of the modeling programs but rather is inherent in the measurement and specification of the loudspeakers. The standard procedure for representing loudspeaker directional response is based on a "black-box" paradigm, wherein most prior knowledge of the loudspeaker's characteristics is ignored. Measurements are taken according to standard procedures and faithfully reported as a *table of data*, which affords the data a defensible claim of objectivity. This paper will demonstrate that modeling accuracy can be significantly improved by incorporating measurable physical parameters into the measurement-and-modeling process – with no loss of objectivity.

Let us consider the physical model inherent in the data table approach. A loudspeaker to be measured is placed on a mechanical rotating device, with the geometric apex of the loudspeaker as close as practically possible to the center of rotation of the turntable [1]. A microphone is then placed at the farthest practical distance, to minimize various error mechanisms, including apparent apex [1], varying microphone distance [2], near-field response anomalies, etc. Frequency response is then measured, normalized to 1 meter, and stored in a two-dimensional table against frequency and turntable angle.

For a given point in a room, the modeling program determines the ray from the speaker's location to the observation point, and the intersection of that ray with the

directional response balloon represented by the data table. It then interpolates the sensitivity from the table, and modifies it by the length of the ray (according to inverse-square law) and by the specified drive signal.

0.2 Directional Point Source Model

The physical model represented by a table of data is a point source with directionality. It is simple to implement and adequate to the task of displaying the approximate projection of the loudspeaker's directional balloon into a room. However, if it is applied to the task of calculating interference, the model is much less satisfactory. Though the interference patterns may be approximately correct for small sources with significant coverage overlap, they are not representative when the sources involved are large relative to the wavelengths of interest (i.e., directional horns).

The results can be greatly improved by storing complex data in the table. This takes account of the electro-mechanical and propagation delays that occur before the wavefront emanates from the supposed point source. It also captures the effect of the source size and shape on the measurement. However, it is important to note that a directional-point-source model is subject to various angular errors and distance-dependence errors, even if the data table contains complex measured data [2]. Some of these will be described in section 3.

0.3 Tessellated Horn Mouth Model

A *tessellated* horn mouth model incorporates the known size and shape of a horn's mouth to create a compound source model. Visualize the wavefront emanating from a horn as a solid surface covered with a mosaic of simple rectangular-shaped tiles. This is an extension of the concept of point-source approximation, but the rectangular tessella is much more computationally efficient, and models can be completed quickly, with far fewer elements.

The technique is not new. In two dimensions, it is described in Olson [3, p. 35] and referenced to a 1930 Wolff and Malter [4] work. Because each chord (the two-dimensional version of a tessella) replaces a large number of point sources, the number of calculations required is greatly reduced. This was an even more critical issue when calculations were performed without computers. Interestingly, the seminal plots of directional characteristics [3], [5], which form the basis of our working understanding of loudspeaker directionality, were originally calculated with this or the more laborious point-source method.

For tessellation models to be accurate, two requirements must be met. Huygens' Principle teaches that the directional pattern is the same whether the source is a vibrating surface or an aperture of the same shape [6]. Consequently, a horn mouth may be modeled as though it were a pulsating surface. However, the principle only holds true if the particle velocity is normal to the surface. In general, this requirement is met by selecting a surface that is equidistant from an original source of sound. This procedure is often referred to as Huygen's Construction [7]. For horn mouth modeling, the shortest path from the horn throat should be used to define the surface.

A second requirement for this method is that all of the output of the source must pass through the defining surface, and propagation away from the surface must be unimpeded (free-field propagation); which is to say that the edges of the radiating surface must be the edges of the mouth. Unfortunately, this requirement eliminates nearly all subject horns because the wavefront they produce does not leave the vertical mouth edges at the same instant that it leaves the horizontal mouth edges. The method can be adapted to such horns, but in the interest of brevity, only two-dimensional experiments will be presented in the current paper.

Because these models capture the physical extent of a source, a model of multiple sources produces valid predictions of interaction, even at observation distances different from that of the original measurement. Precise array predictions are possible, as will be evidenced below by experimental validation.

1.0 MODELING HORN MOUTHS WITH TESSELLATION

1.1 Tessellation Defined

Formally defined, a *tessellation* is a “mosaic - a covering of a geometric surface without gaps or overlaps by congruent plane figures of one type or a few types.” The term has recently come into common use in the field of computer graphics, wherein complex surfaces are graphically rendered by calculating the appearance of each individual tessella and displaying its 3-d projection. For horn mouth modeling, a tessellation will represent the wavefront exiting the mouth of a horn. Only rectangular tessellae will be employed in this paper, though any source shape with known directionality could be used. Fig. 1 illustrates a rectangular tessella.

1.2 Directional Response of Rectangular Tessellae

If a number of point sources are arranged to evenly fill a rectangular planar surface, the directional response of the aggregate source may be calculated by adding the complex contribution of each source. The calculation is accurate to within 1dB if the point-source spacing is smaller than a quarter-wavelength. As the number of points goes to infinity, the directional response of the rectangular source approaches a known, relatively simple, expression. Unlike the point-source array, this expression has no upper frequency limit of validity; and, it can be calculated much faster than a suitably dense point-source model.

The directional response, R_α , of a rectangular source is given in Olson [3, p. 40]:

$$R_\alpha = \left| \frac{\sin[(\pi \cdot l_a / \lambda) \sin \alpha]}{(\pi \cdot l_a / \lambda) \sin \alpha} \frac{\sin[(\pi \cdot l_b / \lambda) \sin \beta]}{(\pi \cdot l_b / \lambda) \sin \beta} \right| \quad (1)$$

where:

l_a and l_b are the dimensions of the rectangle

α is the angle between the normal to the surface of the piston and the projection of the line joining the middle of the surface and the observation point on the plane normal to the surface and parallel to l_a

β is the same as above, with l_b substituted for l_a .

This formula can be expressed in terms of the sinc function, which is $\sin(x)/x$:

$$R_\alpha = \left| \text{sinc}\left[\left(\pi \cdot l_a / \lambda\right) \sin \alpha\right] \cdot \text{sinc}\left[\left(\pi \cdot l_b / \lambda\right) \sin \beta\right] \right| \quad (2)$$

1.3 Tessella Size Requirement

The number of tessellae required for a model is based on the radius of curvature of the modeled source. The largest discrepancy between the tessellated model and the actual source should be smaller than a quarter-wavelength of the highest frequency of interest. Expressed for radius-of-curvature (r_c) and highest frequency of interest, the maximum allowable tessella dimension is:

$$l_{\max} = \sqrt{2cr_c/f} \quad (3)$$

As an example, let's consider the model for a 1 m – wide, 30-degree coverage, high-frequency horn, at 16kHz. The model will require a point-source spacing of no greater than 5.4mm (one quarter of a wavelength at 16 kHz). A two-dimensional model calls for 186 sources. A three-dimensional model will require about 34000 sources. By contrast, a tessellated model will require tessellae of no larger than .289 m, so the mouth can theoretically be modeled as four tessellae in two dimensions, 16 tessellae in three dimensions. Of course, real horns rarely produce simple arced wavefronts with homogeneous source strength and phase. The alert reader will notice that the experimental examples use more tessellae than the calculated minimum.

A tessella source is only valid over its front hemisphere. Applying the equations for angles in the back hemisphere produces results that are identical to the front hemisphere. Physically, the model does not represent a vibrating disk, since the back radiation has the same polarity as the front radiation, and there is no cancellation at 90° off axis. Nor, does it represent a pulsating disk with zero thickness, since that would require a calculation of the diffracted contribution of the opposite side. Quite literally, it is a source model that is only valid over its front hemisphere. Consequently, the valid region of a tessellated model is that angle which is in the front hemisphere of all the sources.

1.4 Generating a Mouth Model

The goal of this new technique is to define a surface that extends from mouth edge to mouth edge and is everywhere perpendicular to the particle velocity. If this condition can be met, then simple-source models may be employed [7, p. 215]. Otherwise, the source models would have to account for the vector part of intensity, which greatly complicates the calculations and is beyond the scope of this paper. For

most real horns, this condition can be met easily for a single cross-section, in two dimensions. But in three dimensions, very few horns can be modeled with a single surface that is both perpendicular to particle velocity and completely encloses the mouth. In order to focus on the simplest application of the concepts, the examples in this paper will be limited to two-dimensional cases.

As mentioned earlier, approximate perpendicularity may be assured by selecting a surface whose points are all equidistant from the source of sound. In the case of a typical horn mouth, part of the surface is defined by line-of-sight to the throat. Near the edge of the mouth, the shortest path to the throat is often curved. This path typically runs along a sidewall for at least part of the distance. Fig. 2 illustrates a family of equal-distance paths for a subject horn. The illustration compares the derived wavefront to a simple arc. The lagging of the edges due to the break in the sidewall is apparent. The wavefront entering the subject horn is assumed to be convex, so the path was plotted from the geometric apex of the walls. If the wavefront entering the horn was known to be flat, the family of paths might have been plotted somewhat differently.

Fig. 3 illustrates the completed tessella model for a real horn of recent design that will be used to illustrate the modeling process. The radius of curvature of the wavefront varies from .65m near the center to about .3m at the mouth edge. This device is intended to be crossed over at 1000 Hz, and has little output above 2500 Hz. By equation 1.1.3, the tessellae must be no larger than 100 mm if the model is to be accurate to 2000 Hz. We will divide the wavefront into 14 equal parts, resulting in tessellae 60 mm wide. Even though the model will only be evaluated in the horizontal plane, we will assign each tessella a height representative of the horn's vertical dimension.

The last tessella has an aiming angle (azimuth) of 39.5° . The angle perpendicular to the tessella is $90^\circ - 39.5^\circ = 50.5^\circ$, so this model is valid within the range -50.5° to $+50.5^\circ$. The response outside this region would be partially composed of back radiation from some or all of the tessellae.

1.5 Implementing the Model

The model is implemented in a program called FChart. This is an object-oriented, Windows-based application written in Visual C++. It is essentially a one-dimensional spreadsheet in which all quantities represent complex frequency response functions. The response curves are displayed on a standardized graph and can be added and multiplied just as real numbers are added and multiplied in a spreadsheet. An FChart document may also include *acoustical* objects, including point sources, circular piston sources, and rectangular tessellae. These objects are located in a virtual acoustical space, within which they can be positioned and aimed. Each acoustical source is "driven" by a transfer function that is expressed as a spreadsheet formula. Several of these acoustical sources can then be grouped together as a single compound source, which can itself be positioned and aimed, and has its own transfer function formula. The sound pressure at any point in the virtual space may be calculated by inserting a *microphone object* at that point. The virtual microphone obtains the complex pressure produced by each individual source at the microphone's location, by equation (2). It then computes the total sound pressure, by applying the principle of superposition. Measured data can also be imported and displayed, for comparison to model predictions.

The rectangular sources that represent the mouth model were created in AutoCAD, and exported to a DXF file (Autodesk “Data eXchange Format”). FChart reads the DXF file and converts any 3DFACE objects it finds to rectangular acoustical source objects. By convention, the location coordinates for a rectangular source represent the center of the rectangle. The width, height, aiming azimuth, aiming elevation, and axial rotation fully describe the physical source and its orientation. Fig. 4 shows a sample FChart screen of a tessellation model, with the dialog box for an individual tessella open.

The computer model is constructed to replicate as precisely as possible the actual measurement setup that was used to measure the directional response of the subject horn. The origin is defined as the center of rotation of the rotator platform. The tessellated mouth model is positioned exactly as the actual device was positioned for the measurement. And, the virtual microphones are positioned exactly as the measurement microphones were positioned. The frequency response measurements of the subject horn are then imported into FChart and are normalized to the axial response. The modeled frequency response predictions are similarly normalized, so that the two families of off-axis curves may be compared.

Fig. 5 shows the comparison of measured vs. modeled magnitude and phase response for 15°, 30°, and 45° off axis. The agreement is within approximately 3dB and 22° of phase, with the general shape of the curves in very close agreement. This indicates that the wavefront model alone captures most of the directional behavior of the horn.

1.6 Optimizing the Model

The wavefront represented by the tessellation is homogeneous in both magnitude and phase, while it may be reasonably assumed that the wavefront produced by a real horn is not homogeneous. At the very least, the tessellae near the mouth edge would be expected to exhibit high frequency roll-off, due to the shadowing of the sidewalls. Also, the arrival time might differ slightly from tessella to tessella, due to the approximate nature of the tessellation technique.

Refinements to the model might be contemplated, based on the expected diffraction through the horn mouth, and possible deviations of the form of the wavefront that entered the throat. It also seems possible that a tessella might be illuminated via multiple paths, resulting in multiple impulses. We chose to evaluate and implement these and other contemplated model refinements by modifying the tessella driving functions (the spreadsheet formulae that modify the contribution of each). A programmed optimizer was then given access to the values in the formulae and directed to minimize the difference between the modeled and measured off-axis response curves. For the examples presented here, it was found that variable gain, delay and low-pass frequency were all that were required to achieve excellent agreement with measured data. Fig. 6 compares the modeled and measured off-axis response after optimization and Table 1 lists the optimized driving functions. Tessellae “A” and “N” are the first and last, respectively: tessellae “G” and “H” are at the center of the mouth. Symmetry is forced by applying the same driving functions to mirror image tessellae. It will be observed that the modeled data matches the measured data to within about 1dB and 10 degrees of phase.

It should be noted that the phase response was not submitted to the optimizer. The precise agreement between measured and modeled phase response is the result of a

physical model that closely represents the real device. Phase response agreement can be used as a qualifying test for a model. If it isn't sufficiently accurate, the model should be re-evaluated and adjusted.

Tessellae	gain (dB)	Delay (us)	2nd-order Bessel LP f (Hz)	Phase at 1kHz (degrees)
A, N	-1.14	19.7	766	-98.7
B, M	-2.15	70.5	2371	-58.2
C, L	-3.9	57.2	2815	-48.2
D, K	-2.3	35.3	1736	-57.3
E, J	0.1	21.2	1708	-52.9
F, I	-0.8	0	1414	-54.3
G, H	0.5	2.2	1408	-55.3

Table 1: Model Refinements for the Driving Functions

As expected, the mouth-edge tessellae have significant high-frequency roll-off, due to the shadowing of the sidewalls. A smooth progression of delays results until reversing at tessellae “A” & “N”. This is surprising until the phase response is considered. The phase response of the low-pass filter combines with the phase lag due to delay, to produce a smooth progression of phase response across the mouth.

These results represent the directional behavior of the horn only. All that remains to complete the model is to select a driving function for the overall model that matches the measured frequency response. After arbitrarily setting the driving function to force the 15-degree off-axis curves to be equal, the curve families appear as in Fig. 7. The pairs of curves (measured vs. modeled) represent 0°, 15°, 30°, & 45° off axis.

2.0 MODELING ARRAYS WITH TESSELLATION

2.1 A Two-Horn Model

Let us consider an array of two of the horns modeled in Section 1. Within FChart, this is accomplished by creating a compound source object from the optimized model of the horn. The array of two horns is modeled by duplicating the compound source and changing the coordinates and aiming angles of the two horns. A graphical depiction of the model is given in Fig. 8.

Fig. 9 shows the absolute response, modeled and measured, at 0°, 10°, 20°, and 30°. The agreement between model predictions and measured data is very good. In fact, the magnitude of discrepancy is comparable to the unit-to-unit variation of the modeled devices.

2.3 Angular Region of Validity

The compound model is valid wherever both individual models are valid. In the example, each model is valid from -50.5° to $+50.5^\circ$. The horns are each splayed 25° from the centerline, so the valid regions are from -71° to $+25.5^\circ$, and -25.5° to $+71^\circ$. The region of intersection is only -25.5° to 25.5° . Note that this region only represents the

range over which excellent results can be guaranteed. In practice, we will see that the models produce valid predictions considerably beyond the valid region.

The directional response of an individual tessella in the back hemisphere is the mirror image of its directional response in the front hemisphere. So, for example, the response at 95° off axis is the same as the response at 85° off axis. However, if the tessella is relatively small, its response will be like that of a point source over most of its frequency range. The tessella will exhibit directionality only at the upper end of its frequency range. At high frequencies, most of the sound pressure in a given direction is supplied by the tessellae that are aimed in that direction. The contribution of tessellae aimed approximately 90 degrees to the direction is very small. Consequently, the models are accurate over a broader range than expected.

Let's see how the example models perform outside the known-good angular region. Fig. 10 shows the absolute response of a single horn, modeled and measured, at 0° , 60° , 75° , and 90° . The modeled response at 60° is very accurate down to 300 Hz, and within 2 dB below 300 Hz. Significant errors begin to appear at 75 degrees.

Fig. 10 shows the absolute response of two horns, modeled and measured, at 0° , 40° , 60° , and 80° . The agreement is very good at 40° . Significant errors begin to appear at 60° . If we take -75° to 75° as the valid range for a single horn, then the splayed horns in the two-horn model should be valid from -100° to 50° , and -50° to 100° , respectively. The region of intersection is -50° to 50° . This correlates well with observation of Fig. 11.

3 CONCLUSIONS

3.1 Benefits

3.1.1 Immunity from Geometric Errors

The data-table approach is subject to several error mechanisms, the most familiar of which is apparent apex error [1]. Apparent apex error is defined as the error in the computed beamwidth that occurs if the apex of the beam is not at the center of rotation. More generally, apparent-apex theory explains the issue of angular errors that are due to the finite size of the source.

A directional-response data table is a record of the response that was measured at each of the standard rotator positions. For instance, the data recorded for 45° is the measurement that was taken with the rotator turned 45° off axis. As long as we keep in mind that the “ 45° ” label represents the rotator position – not the speaker-referenced off-axis angle, then there is no error in the data acquisition process.

However, the acoustical path from the source to the microphone was not 45° off the axis of the horn being measured; so apparent apex errors occur when a modeling program uses the 45° rotator-position data to estimate the 45° speaker-referenced response. Fig. 12 illustrates.

With a tessellated model, the 45° measurement is only used to “train” the model, so that it will accurately predict the response at that microphone position. If the acoustical path during the measurement was actually 50° off the axis of the speaker (as in Fig. 12), then it is also 50° off the axis of the tessellated model. Rather than referring angles and

distances to the rotator center and angle, angles and distances are determined by the absolute position and aiming of the individual tessellae. When the far-field response at 45° is required, the tessellated model calculates it correctly.

There are two other errors that result from the geometry of the measurement setup. A reduction in SPL occurs as the horn mouth rotates away from the [2]. This type of error is minimized by employing long measurement distances, and by rotating about the mouth of the horn, rather than the apex of the horn walls. Unfortunately, this is in conflict with the requirement for reducing apex error at the edge of the beam.

The other error is primarily of interest for modeling arrays. It has been referred to as focal error because it affects the formation of a beam at long distances. The main component of phase that governs arrays of sources is the propagation time. For correct results, the source location specified in the model must coincide with the point about which the source was rotated, for the measurement. Otherwise, the variation of propagation time with angle will not match that of the measurement. Unfortunately, standard practice is for the source location to represent some identifiable physical detail, such as the center of the baffle; which is rarely located at the center of rotation.

Even if the source is correctly positioned, there is a residual propagation time error that results from the angular error. Referring to Fig. 12 and the 45° rotator-position, the path from the source to the microphone is slightly longer because of its 5° angular error. The path-length error is (path length) * (1-cos(5°)), or about .023 m in this example. In the far field, the source's contribution will arrive 63 microseconds earlier than expected. This amount of variation is insignificant for the midrange device in the example, but it can be critical for arrays of high-frequency devices [8].

Tessellated mouth models are immune to all the geometrical errors described above.

3.1.2 Frequency and Angle Resolution

The tessellated model is not strictly a model, because it has been perturbed to obtain agreement with measured data. In fact, it is helpful to think of it as “intelligent interpolation”, rather than modeling. By using a priori knowledge of the source, we can estimate the response between measurement points much more intelligently. For an indication of how precise the estimates can be, refer to Fig. 7. This graph depicts the predicted and modeled data for 0°, 15°, 30°, and 45°. However, only the 0°, 10°, 20°, and 30° curves were used by the optimizer. The 15° curve is an interpolated point, and the 45° curve is an extrapolated point!

For this example and similar devices, the response for any point within the valid angular range can be estimated with accuracy comparable to that of the original measurements. Furthermore, the results have the same frequency resolution as the original measurements. There has been no smoothing for conversion to fractional-octave-band data, so calculations of interference can be performed with full frequency resolution. The smoothing and conversion to octave-band data is left to the end.

3.2 Limitations and Future Developments

3.2.1 Limited Angular Range

The primary limitation of the method is that the tessellation model is only valid over a limited angular range. For some applications, this restriction is not problematic. We can simply constrain our use of the model to the valid range. However, if the technique were introduced, with this restriction, into commercial acoustical modeling programs, the utility of the programs would be unreasonably restricted.

However, the region of the model that is not accurately modeled is actually of much less interest than the region that is accurately modeled. We are of course much more interested in the performance of the beam of coverage than the back-side spillage. One might reasonably build a compound model, which uses the best known method for each angle. Within the valid angle, the results would be drawn from the tessellated model. Outside the valid angle, the results would be drawn from the next-best interpolation method. The modeling results would be no worse than the current standard at any angle, and would be significantly improved in the primary coverage beam of the device.

It would also be possible to store multiple tessellation models, each of which is constructed and optimized for a different angular range. Due to the lower priority of back-axis radiation, however, the extra effort that would be involved is probably not warranted.

The most desirable course of improvement is to extend the unified model with consideration of diffraction and shadowing. Research is currently under way to develop practical techniques for modeling horn walls and edges.

3.2.2 Geometrical Requirements

The technique, as described here, is only applicable to symmetrical devices, due to the requirements stated in section 1.3. And of course, we have only treated 2-dimensional cases in this paper. The process can be extended to 3-dimensions and asymmetrical devices through one of several approaches. The approach selected will depend on the characteristics of the particular device under test. A second paper is contemplated, which would address various 3-dimensional approaches.

3.2.3 Diffraction and Shadowing, Modifying Functions

Differences between predicted and measured array response may be attributed to various factors, all of which result from the introduction of an additional source. There may be reflections and diffractions off of, or shadowing by the adjacent structure. The mutual coupling of the sound sources may change their individual contributions. And there may be a baffling effect, wherein adjacent structures reduce the back-radiation of the first source and affect its acoustical loading. In the Loudspeaker Arrayability Research Group (LARGE) proposal by AES working group SC-04-03, these effects are referred to as modifying functions.

The example related here was for a “good horn”, which was specifically designed to array well. Less-well-behaved horns might require more complex modeling. Furthermore, the array that was examined followed “best practices” for arraying horns. The sources were tight-packed, mouth-edge to mouth-edge, so there was no obstruction

of line-of-sight to the horn mouths. Consequently, the effects of shadowing and reflections from adjacent devices are negligible. That these effects are negligible was not an up-front assumption, but was determined by specific experiments.

First, a single horn was measured. Then the measurement was repeated with a second horn placed next to it, but not driven. The difference between the two measurements was always less than 0.3 dB. By subtracting the response with the adjacent horn present from the response without the adjacent horn, a residual response was calculated. This residual was more than 25 dB down at all frequencies. To evaluate mutual coupling issues, the horns were placed together and measured individually, then with both horns driven. Then the sum of the individual horn measurements was compared to the measurement of both. There was never more than a 0.2-dB difference.

These measurements were all made in the known-valid angular range. It is reasonable to assume that, further off axis, diffraction and reflection will become increasingly significant. If the technique is extended to the back hemisphere, then of course shadowing will also become significant. Furthermore, other types of sources such as direct-radiators and smaller horns are more interactive, and it is very possible that modifying functions would be required to obtain sufficient accuracy, when modeling arrays of these devices.

3.3 Applications

The modeling techniques described in this paper were developed to support the arraying and processing of three specific loudspeaker systems. In all three cases, only the vertical directionality was an issue with regard to processing; so there was no need for a three-dimensional model. Also in all three cases, the various sources are aimed in approximately the same vertical direction; so the valid angular region for the array is not much smaller than that of an individual device. The purpose of the modeling is to optimize the performance within the intended coverage pattern, so the valid angular range is more than adequate.

In the case of the first system, array calculations were a necessity arising from the goals of the design. In order to obtain a 12-dB increase in high-frequency projection, five to eight horns are packed tightly together, and then processed separately – so that a useful beam-shape may be formed. Likewise, an array of three or six mid-frequency horns is processed to produce a beam matching that of the high-frequency array. The technique for deriving the signal-processor settings utilizes the same program, FChart, and is described in detail in [9]. Because the measurement process used for the mid-frequency and high-frequency sections cannot resolve sufficiently low frequencies, a tessellated model is used for the low frequency section. Once the tessellation technique has been proven for asymmetrical sources, it will be applied to the entire system. At that point, the modeling process will become part of a computer control system, which users will employ for on-site calibration and adjustment of the system.

The second system is a portable concert speaker that is deployed in curved vertical arrays. It differs from the other applications described here in that its rigging system allows the selection of small angular increments. Using a complete tessellation model of all three sections, optimal rigging angles were determined for various numbers

of cabinets and shapes of venues, and optimum signal-processor settings were developed for each configuration.

The third system is a three-way, coaxial loudspeaker in a single cabinet. In its most common configuration, these cabinets are “dead-hung” (all boxes level) 1 to 5 rows high, typically with a down-tilted version of the cabinet in the bottom row. FChart modeling has been used to optimize the transition from the standard cabinet to the down-tilted cabinet, as well as for evaluating new array designs and their applicability to unusually shaped venues.

4 REFERENCES

- [1] M. S. Ureda, “Apparent Apex Theory,” presented at the 61st Convention of the Audio Engineering Society, 1978, Preprint #1403.
M. S. Ureda, “Apparent Apex Revisited”, 1991, Preprint #3040.
M. S. Ureda, “Apparent Apex, Part III: The Three-Dimensional Case”, 1991, Preprint #3166.
M. S. Ureda, “Apparent Apex, Part IV: Direct Radiators”, 1992, Preprint 3324.
M. S. Ureda, “Apparent Apex”, 1997, Preprint #4467.
- [2] D. W. Gunness, “Loudspeaker Directional Response Measurement,” presented at the 89th Convention of the Audio Engineering Society, 1990, Preprint #2987.
- [3] H. F. Olson, *Elements of Acoustical Engineering* (Van Nostrand, New York, 1947).
- [4] I. Wolff and L. Malter, “Jour. Acous. Soc. Amer.”, Vol.2, No. 2, p. 201, 1930.
- [5] L. L. Beranek, *Acoustics* (McGraw-Hill, New York, 1954).
- [6] Lord Rayleigh, *Theory of Sound, Vol. II* (MacMillan & Co., London, 1896)
- [7] A. D. Pierce, *Acoustics* (Mc-Graw Hill, 1981) p. 175.
- [8] D. W. Gunness & J. F. S. Speck, “Phased Point Source Technology and the Resultant KF900 Series,” (Eastern Acoustic Works, Inc., 1997).

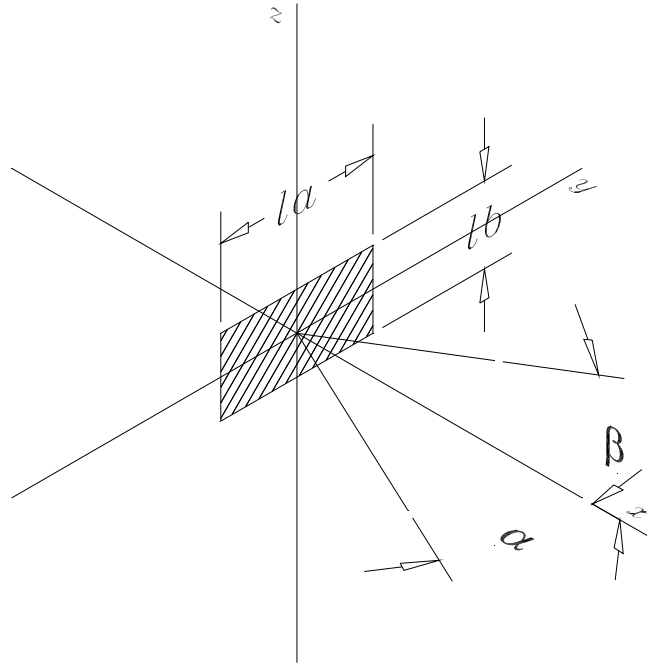


Fig. 1: Rectangular Tessella Nomenclature

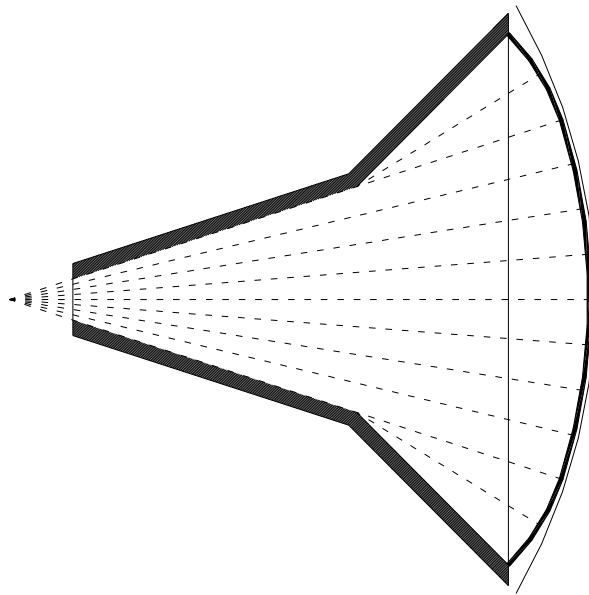


Fig. 2: Lines of equal distance (Huygen's Construction)

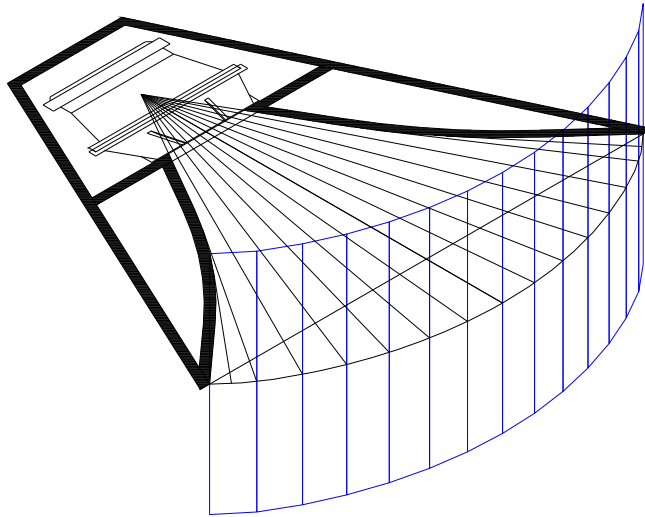


Fig. 3: Tessellated Mouth Model

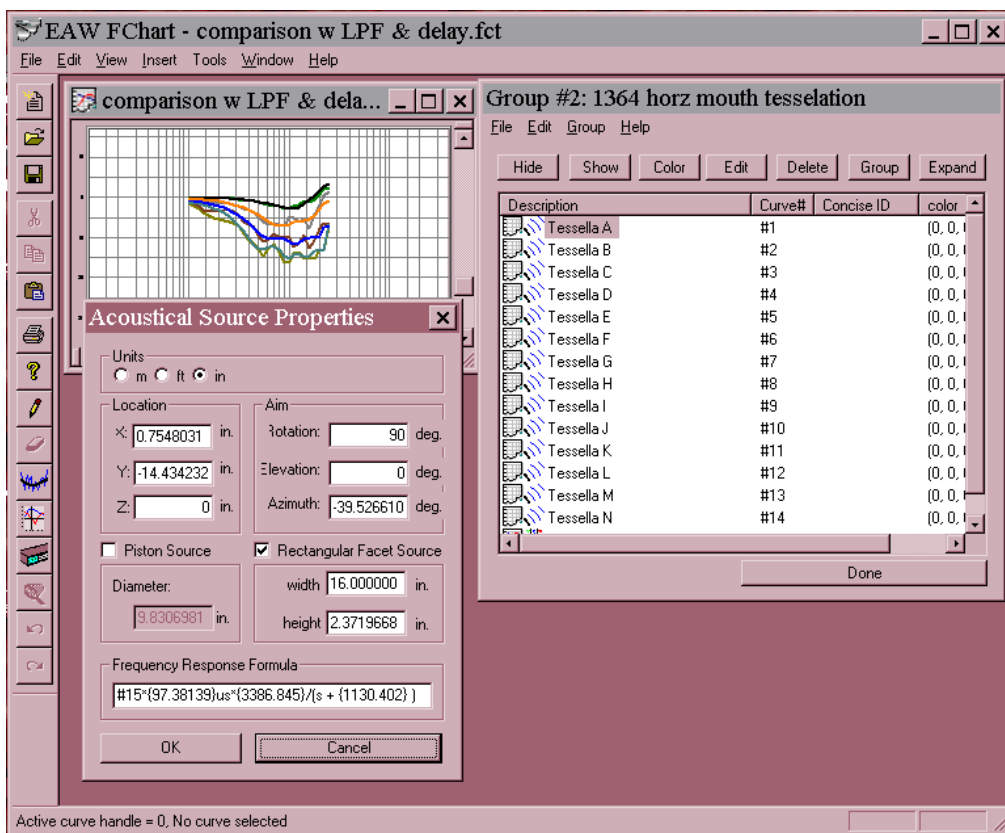


Fig. 4: FChart Tessellation Model Interface

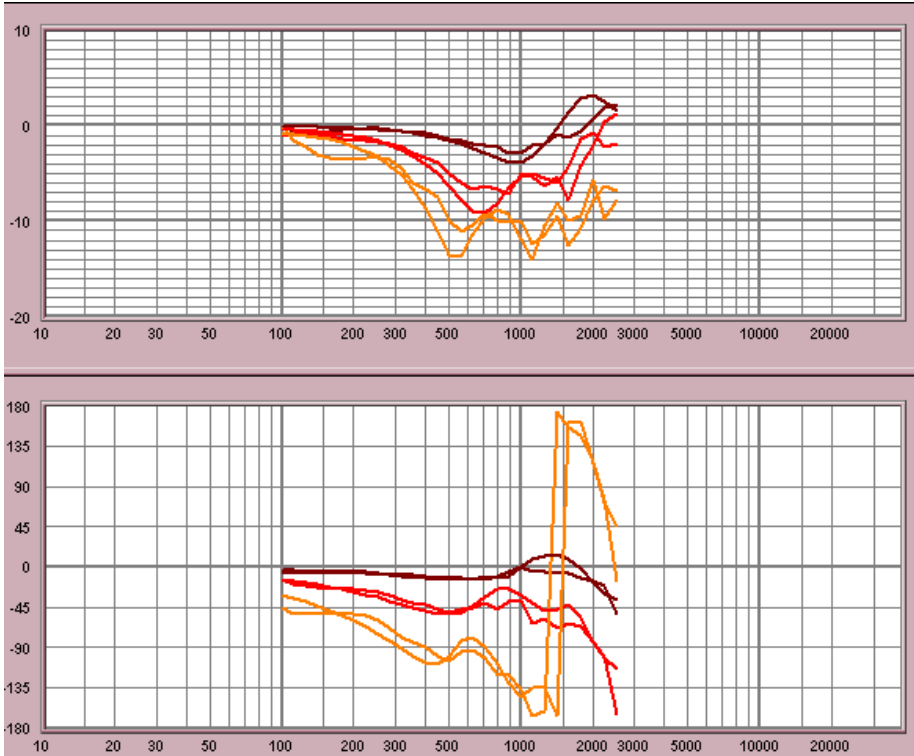


Fig. 5: Measured Response vs Un-Optimized Mouth Model (15°, 30°, and 45°).

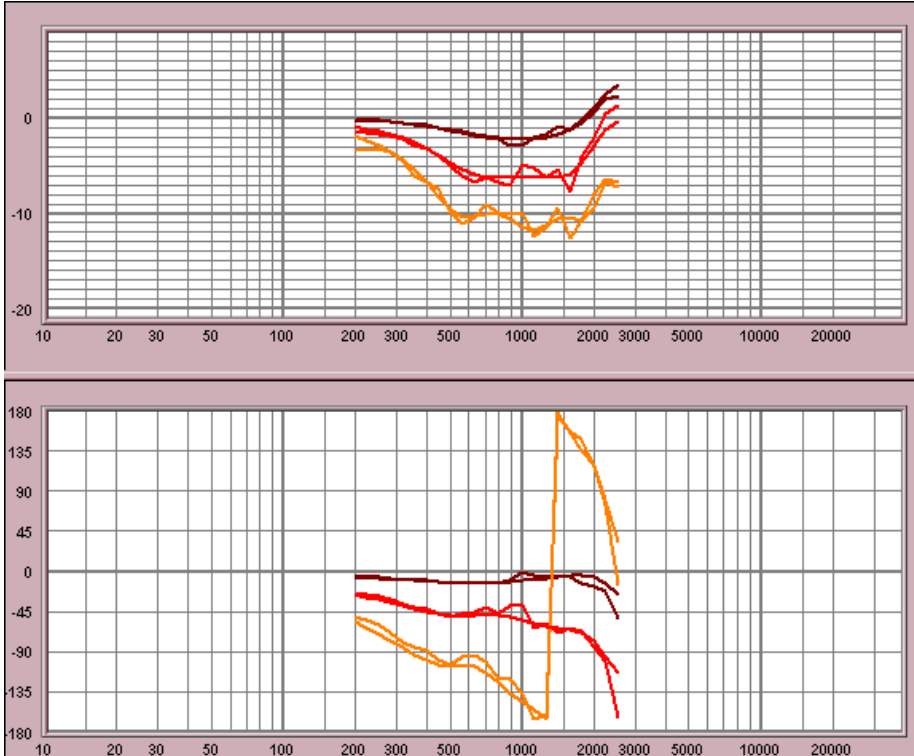


Fig. 6: Optimized Model vs. Measured Directional Response (15°, 30°, and 45°).

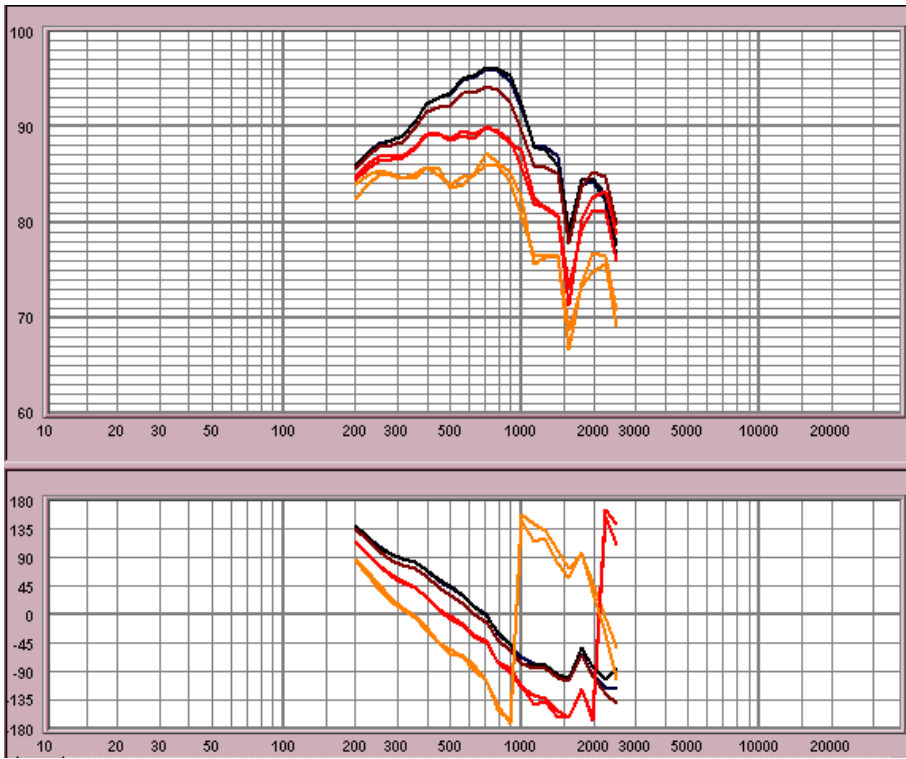


Fig. 7: Optimized Model vs. Measured Absolute Response (0° , 15° , 30° , and 45°).

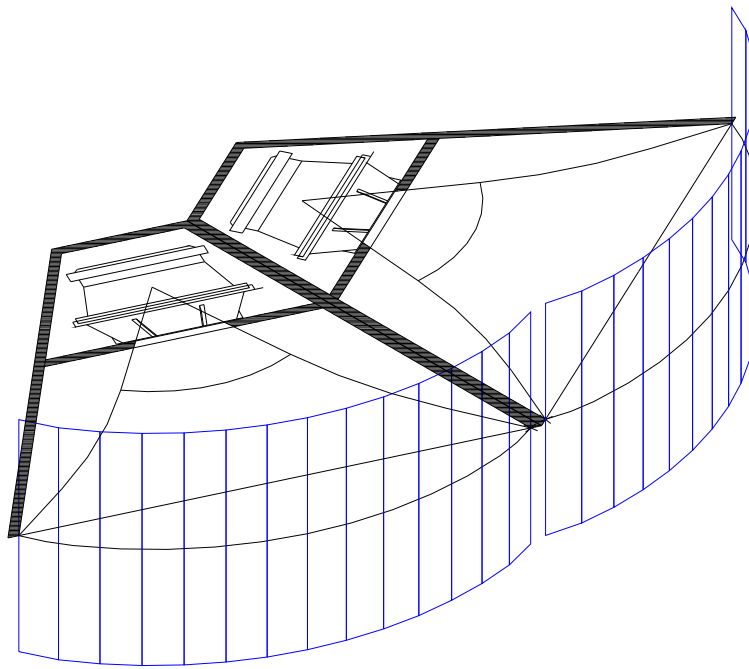


Fig. 8: Two-Horn Model, made up of two Compound Sources

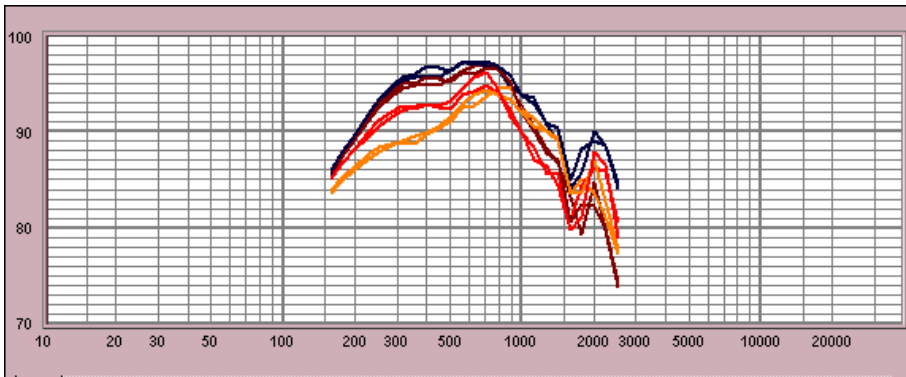


Fig. 9: Modeled vs. Measured for array of two horns (0° , 10° , 20° , and 30°)

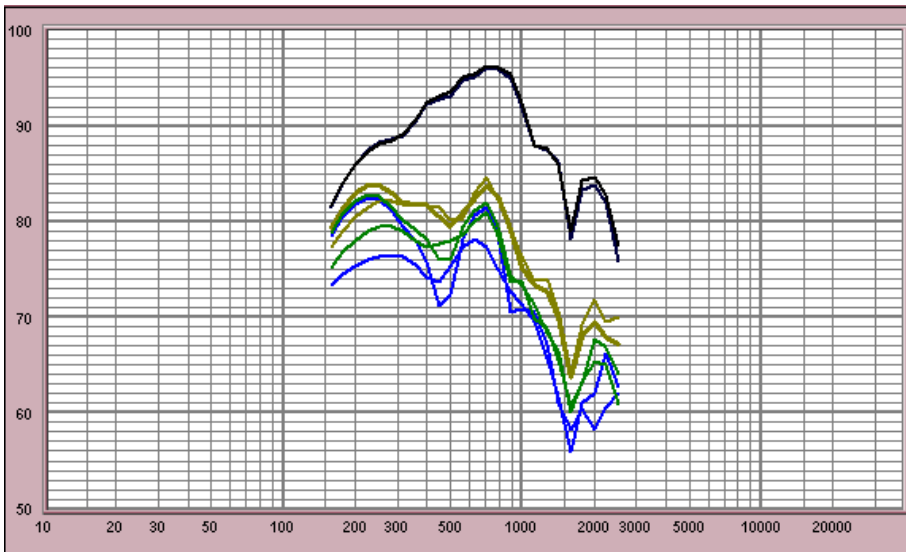


Fig. 10: Single horn model, outside valid angular range (0° , 60° , 75° , and 90°).

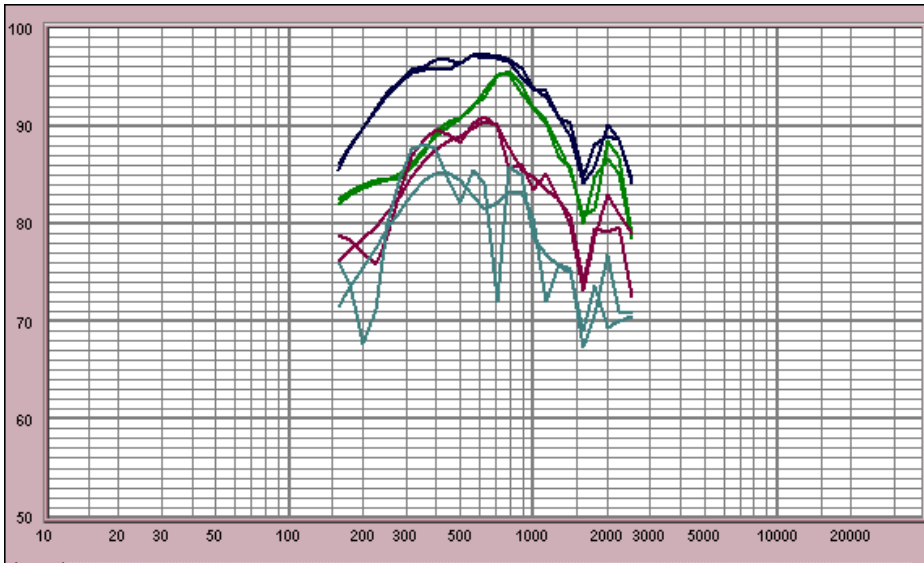


Fig. 11: Two-horn model, outside valid angular range (0° , 40° , 60° , and 80°).

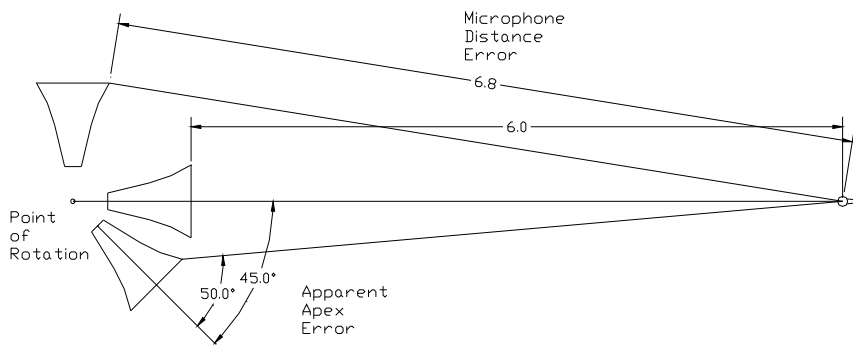


Fig. 12: Angular and Distance Errors